



Mapping Motor Pathways in Parkinson's Disease Patients with Subthalamic Deep Brain Stimulator: A Diffusion MRI Tractography Study

Yan Li · Naying He · Chencheng Zhang · Yu Liu · Jun Li ·
Bomin Sun · Yijie Lai · Hongyang Li · Chengyan Wang ·
Ewart Mark Haacke · Fuhua Yan · Dianyou Li

Received: November 18, 2021 / Accepted: January 24, 2022 / Published online: February 14, 2022
© The Author(s) 2022

ABSTRACT

Introduction: This study assessed the safety of postoperative diffusion tensor imaging (DTI) with on-state deep brain stimulation (DBS) and the feasibility of reconstruction of the white

Yan Li and Naying He have contributed equally to this work.

Supplementary Information The online version contains supplementary material available at <https://doi.org/10.1007/s40120-022-00331-1>.

Y. Li · N. He · Y. Liu · E. M. Haacke · F. Yan (✉)
Department of Radiology, Ruijin Hospital, Shanghai Jiao Tong University School of Medicine, No. 197, Ruijin 2nd Road, Huangpu District, Shanghai 200025, China
e-mail: yfh11655@rjh.com.cn

C. Zhang · B. Sun · Y. Lai · H. Li · D. Li (✉)
Department of Neurosurgery, Center for Functional Neurosurgery, Ruijin Hospital, Shanghai Jiao Tong University School of Medicine, No. 197, Ruijin 2nd Road, Huangpu District, Shanghai 200025, China
e-mail: ldy11483@rjh.com.cn

J. Li
School of Information Science and Technology, ShanghaiTech University, Shanghai, China

C. Wang
Human Phenome Institute, Fudan University, Shanghai, China

E. M. Haacke
Department of Radiology, Wayne State University, Detroit, MI, USA

matter tracts in the vicinity of the stimulation site of the subthalamic nucleus (STN). The association between the impact of DBS on the nigrostriatal pathway (NSP) and the treatment effect on motor symptoms in Parkinson's disease (PD) was then evaluated.

Methods: Thirty-one PD patients implanted with STN-DBS (mean age: 66 years; 25 male) were scanned on a 1.5-T magnetic resonance imaging (MRI) scanner using the DTI sequence with DBS on. Twenty-three of them were scanned a second time with DBS off. The NSP, dentato-rubro-thalamic tract (DRTT), and hyperdirect pathway (HDP) were generated using both deterministic and probabilistic tractography methods. The DBS-on-state and off-state tractography results were validated and compared. Afterward, the relationships between the characteristics of the reconstructed white matter tracts and the clinical assessment of PD symptoms and the DBS effect were further examined.

Results: No adverse events related to DTI were identified in either the DBS-on-state or off-state. Overall, the NSP was best reconstructed, followed by the DRTT and HDP, using the probabilistic tractography method. The connection probability of the left NSP was significantly lower than that of the right side ($p < 0.05$), and a negative correlation ($r = -0.39$, $p = 0.042$) was identified between the preoperative symptom severity in the medication-on state and the connection probability of the left NSP in the

DBS-on-state images. Furthermore, the distance from the estimated left-side volume of tissue activated (VTA) by STN-DBS to the ipsilateral NSP was significantly shorter in the DBS-responsive group compared to the DBS-non-responsive group ($p = 0.046$).

Conclusions: DTI scanning is safe and delineation of white matter pathway is feasible for PD patients implanted with the DBS device. Postoperative DTI is a useful technique to strengthen our current understanding of the therapeutic effect of DBS for PD and has the potential to refine target selection strategies for brain stimulation.

PLAIN LANGUAGE SUMMARY

For some more seriously affected Parkinson's disease (PD) patients, drugs are no longer effective in treating their symptoms. An alternate treatment is to use deep brain stimulation (DBS), a commonly used neurosurgical therapy for PD patients. For those DBS treatments targeting the subthalamic nucleus (STN), the electrical stimulation used may impact nearby white matter tracts and alter the effectiveness of the DBS treatment. The nigrostriatal pathway (NSP), dentato-rubro-thalamic tract, and hyperdirect pathway are three white matter tracts near the STN. They are all relevant to motor symptoms in PD. This study examined whether imaging these tracts using magnetic resonance imaging (MRI) is safe and feasible in the presence of DBS leads. The relationships between the fiber-tracking characteristics and distance to the DBS leads were then evaluated. For this purpose, 31 PD patients with stimulation-on were scanned on a 1.5 T MRI scanner using a diffusion tensor imaging sequence. A total of 23 subjects underwent another scan using the same sequence with stimulation-off. No adverse events related to diffusion tensor imaging were found. Among the white matter tracts near the STN, the NSP was best delineated, followed by the dentato-rubro-thalamic tract and the hyperdirect pathway. The connection probability of the left NSP was significantly lower than that of the right side as were

the subject's motor symptoms. The closer the distance between the NSP and the stimulation location, the better the DBS outcome. These findings indicate that imaging white matter tracts with DBS on is safe and useful in mapping DBS outcomes.

Keywords: Postoperative imaging; Diffusion tensor imaging; Parkinson's disease; Deep brain stimulation; Subthalamic nucleus; White matter fiber tracts

Key Summary Points

White matter tracts near the deep-brain-stimulation (DBS) site were reconstructed based on a 10-min diffusion tensor imaging sequence acquired on a 1.5-T magnetic resonance imaging (MRI) scanner, and no adverse events were identified in either DBS-on or DBS-off states.

In the Parkinson's disease (PD) patients implanted with the subthalamic deep brain stimulator, the nigrostriatal pathway (NSP) was best reconstructed, followed by the dentato-rubro-thalamic tract (DRTT) and hyperdirect pathway (HDP), using the probabilistic tractography method.

The connection probability of the left NSP was significantly lower than that of the right side, and a negative correlation was identified between the preoperative symptom severity in the medication-on state and the connection probability of the left NSP in the DBS-on-state images.

Clinically effective DBS electrodes for alleviation of PD motor symptoms were in close anatomical proximity to the left-side NSP.

INTRODUCTION

Deep brain stimulation (DBS) of the subthalamic nucleus (STN) is an effective neurosurgical therapy for the treatment of advanced, levodopa-responsive Parkinson's disease (PD). However, DBS-induced improvement of motor function varies greatly in individual patients [1–3]. One possible mechanism underlying the variation in treatment effect is related to the influence of STN-DBS on the white matter bundles near the stimulation site [4, 5]. According to previous studies, the white matter tracts in close proximity to the STN, particularly the nigrostriatal pathway (NSP), dentato-rubrothalamic tract (DRTT), and hyperdirect pathway (HDP), are related to the control of motor behavior, the pathophysiology of PD, and potentially the therapeutic mechanism of DBS [6–8]. The NSP, which connects the substantia nigra (SN) with the dorsal striatum, is a crucial pathway in the basal ganglia that influences voluntary movement, and the loss of dopamine neurons in this pathway is one of the main pathological features of PD [7, 9]. Modulation of the DRTT is responsible for the therapeutic effects of DBS that lead to the alleviation of tremor [6]. The HDP, which directly connects the motor-related cortical areas and the STN [10], is thought to be associated with DBS-induced clinical improvement, and damage to the tract may be responsible for motor symptoms or other movement disorders such as ataxia or tremor [8].

Previous studies have shown that the distance between DBS electrodes and specific white matter tracts in the patients may affect the effectiveness of DBS [4]. However, so far, most magnetic resonance imaging (MRI) studies examining the relationship between the DBS-induced therapeutic effect and the DBS-influenced white matter tracts have only been performed on open-access datasets, such as the Human Connectome Project (HCP) and Parkinson's Progression Markers Initiative (PPMI), or on patient images acquired before DBS surgery [11, 12]. The degeneration and integrity of the tracts need to be examined in patients postoperatively, because the impaired

integrity of white matter bundles after the implantation of the DBS device or the degeneration of the white matter tracts years after surgery may potentially account for the variation and alteration in DBS effects [13]. To date, there is no known study reporting the level of degeneration and integrity of white matter tracts after DBS surgery. Therefore, it would be of great interest to delineate the white matter tracts after DBS surgery [14]. The pathways shown by diffusion tensor imaging (DTI) can help further elucidate the mechanisms of DBS and further guide therapy. With the help of postoperative DTI tractography, the role of the white matter pathways in DBS for the treatment of PD can be further studied [15].

Safety and feasibility issues need to be validated for the DTI sequence after DBS implantation. There is evidence supporting the safety of postoperative MRI, but the most commonly used sequences have been T1-weighted, T2-weighted, proton density-weighted, and gradient-echo imaging. These methods are mainly used to confirm the location of electrodes and to check for possible surgical complications [16–18]. DTI-based tractography allows non-invasive mapping of the structural connections of the brain. Preliminary postoperative diffusion-weighted tractography conducted by Muller and colleagues [15] was shown to be both safe and feasible in the DBS-off state, but it has not been reported whether it is safe to scan the DTI sequence in the DBS-on state and whether the results of tract reconstruction are affected by the DBS states or different tractography approaches, including the deterministic tractography (DT) and the probabilistic tractography (PT) methods. It would benefit patients to undergo MRI scanning with DBS on, since it may be uncomfortable (e.g., excessive tremor, unpleasant subjective feeling) for some patients to undergo MRI scanning with DBS switched off. Furthermore, given that the access to MR scanners in most clinical centers is limited, the long acquisition time of the DTI sequence proposed by Muller and colleagues [15], which takes about 25 min, may hinder its clinical application. They chose a long repetition time (25,000–28,000 ms) to maintain low specific absorption rate (SAR) values out of safety

concerns. However, it would be an advantage if the scanning time could be shortened without exceeding the safety range of the SAR value or sacrificing the image quality.

The primary aim of the present study was to validate the safety and feasibility of the delineation of white matter bundles near the stimulation site of STN-DBS based on clinically applicable postoperative DTI sequences acquired from a 1.5-T scanner within a relatively short amount of time (about 10 min). We shortened the total acquisition time by setting a relatively short repetition time (6500 ms) while keeping the SAR value under the recommended threshold level (0.4 W/kg) [19]. Furthermore, we examined whether the NSP, DRTT, and HDP tracts could be delineated using both DT and PT approaches and quantitatively assessed the effect of DBS state (DBS-on and DBS-off) on the tractography results. Finally, we also evaluated and interpreted the relationships between the characteristics of reconstructed white matter tracts and the clinical assessment of PD symptoms and the DBS effect.

METHODS

This study was approved by the Ruijin Hospital Institutional Review Board (Approval Number: 2018017). All procedures in the present study were in accordance with the Declaration of Helsinki. Each patient was informed of the procedures of the study and signed a consent form.

Patient Inclusion

From August 2020 to December 2020, a total of 43 PD patients implanted with bilateral quadripolar DBS electrodes (Model 3387, Medtronic, Minneapolis, MN; L302, PINS, Beijing; Model 1210, SceneRay, Suzhou) were recruited for MRI scanning. All the patients were right-handed. Twelve patients were excluded from the scanning, as follows: seven patients declined to participate, two were excluded due to MRI contraindications, and the other three were excluded because their DBS electrodes were at globus pallidus interna (GPi) instead of

STN. Therefore, 31 patients underwent scanning with the DBS device on, and then 23 of them were rescanned using the same MRI protocol after turning off the DBS device for about 1 h. Eight patients did not undergo the second scan: three patients refused to turn off the DBS, and the other five were unable to complete the second MRI scan because their symptoms of tremor became too severe after turning off the DBS device. The flowchart for the study and the population recruitment process is shown in Fig. 1.

Image Acquisition

Preoperative MR images (T1-weighted and T2-weighted images) were obtained from each patient before the day of DBS surgery on a 3.0-T scanner (Ingenia, Philips, Best, Netherlands). The acquisition parameters for T1-weighted images were as follows: repetition time (TR) = 7.1 ms, echo time (TE) = 3.4 ms, flip angle = 7°, voxel resolution = $0.75 \times 0.75 \times 1.5 \text{ mm}^3$, matrix = 320×320 , number of slices = 150, bandwidth (BW) = 241 Hz/px, acquisition time (AT) = 3 min 14 s. The acquisition parameters for T2-weighted images were as follows: TR = 4000 ms, TE = 106 ms, flip angle = 90°, voxel resolution = $0.75 \times 0.75 \times 1.5 \text{ mm}^3$, matrix = 320×320 , number of slices = 100, BW = 439 Hz/px, AT = 5 min 36 s.

During the week after surgery, helical computed tomography (CT) imaging (IQon Elite Spectral CT, Philips, Best, Netherlands) was performed axially (tube current = 235 mA; voltage = 120 kV; in-plane voxel resolution = $0.5 \times 0.5 \times 5 \text{ mm}^3$). The postoperative CT images were fused to the preoperative MR images to estimate the volume of tissue activated (VTA) by DBS using the Lead-DBS toolbox (www.lead-dbs.org, version 2.5.2), which indicates a rough approximation of the surrounding tissue influenced by DBS [20].

Postoperative MRI was performed on a 1.5-T MR scanner (Magnetom Aera, Siemens Healthcare, Erlangen, Germany) using a 16-channel head coil. The scanning protocol is summarized in Table S1. The complete DTI sequence

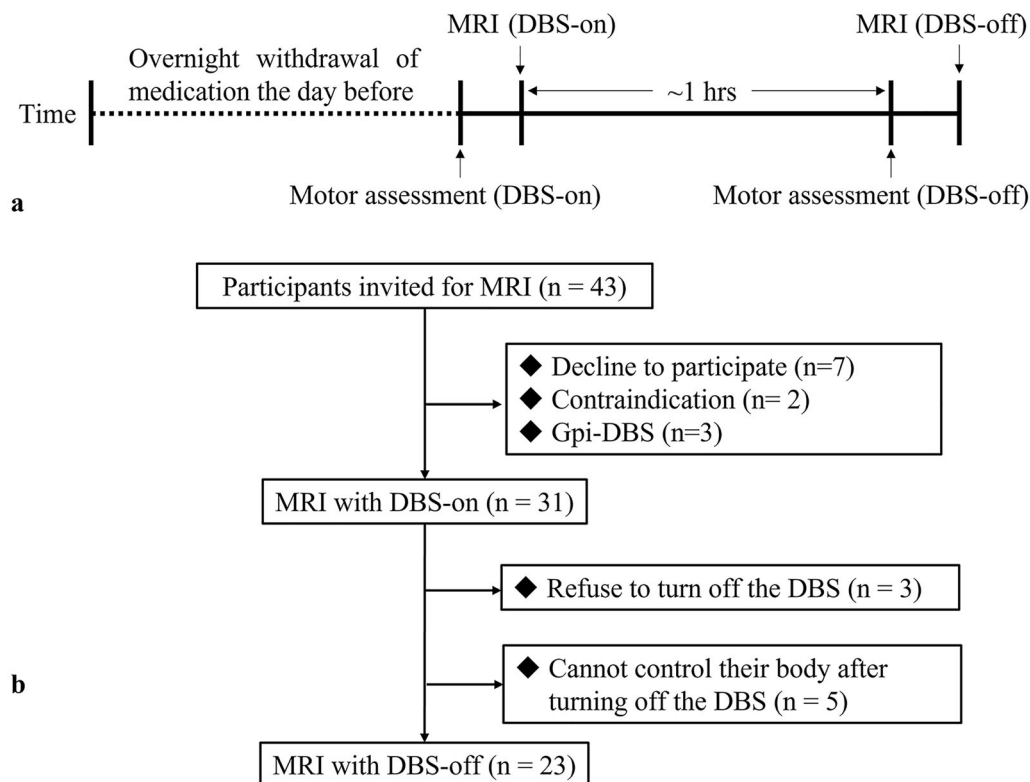


Fig. 1 Study procedure and patient inclusion. **a** Study procedure; **b** flowchart of patient recruitment

consisted of 64 diffusion-weighted directions with $b = 1000 \text{ s/mm}^2$ and 16 interspersed scans with $b = 0 \text{ s/mm}^2$. The other acquisition parameters were as follows: TR = 6500 ms, TE = 126 ms, matrix = 110×110 , voxel size = $2 \times 2 \times 2 \text{ mm}^3$, BW = 1336 Hz/px, AT = 9 min 13 s, and SAR = $0.34 \pm 0.02 \text{ W/kg}$. Sagittal high-resolution 3D T1-weighted structural images were acquired to define the regions of interest (ROI) for fiber tracking. A magnetization-prepared rapid-acquisition-gradient-echo (MPRAGE) sequence was used with the following parameters: TR = 3400 ms, TE = 3 ms, inversion time = 900 ms, flip angle = 8° , matrix = 216×224 , voxel size = $1 \times 1 \times 1 \text{ mm}^3$, BW = 260 Hz/px, AT = 6 min 2 s, and SAR = $0.03 \pm 0.004 \text{ W/kg}$.

The date of the postoperative MRI, time since DBS surgery, and incidence of any adverse events related to MR scanning were recorded. The clinical data of the patients are summarized in Table 1.

Image Quality Assessment

A trained MRI analyst conducted a visual image quality assessment [21] by inspecting all 80 volumes for each DTI scan. Any volume that appeared to contain artifacts was marked and discarded. The corresponding b-values file and the diffusion gradient table documents were modified accordingly.

Region of Interest Selection

The NSP was defined as the connection between the SN and corpus striatum (STR). Streamlines seeded from the dentate nucleus (DN) to the contralateral thalamus (THA) were estimated as the DRTT. Streamlines from the precentral gyrus (PG) to the STN were estimated as the HDP [15]. The bilateral ROIs in Montreal Neurological Institute (MNI) space (STN, STR, and SN) were extracted from the ATAG-elderly atlas [22]; DN was extracted from the delineation by He and colleagues [23]; THA and PG were

Table 1 Demographics and clinical information of the patients

	DBS-on (<i>n</i> = 31)	DBS-off (<i>n</i> = 23)
Age (years)	66 ± 6	67 ± 5
Male sex, no. (%)	25 (80.6%)	18 (78.3%)
DBS type	Medtronic (<i>n</i> = 24) PINS (<i>n</i> = 1) SceneRay (<i>n</i> = 6)	Medtronic (<i>n</i> = 17) PINS (<i>n</i> = 1) SceneRay (<i>n</i> = 5)
Disease duration (years)	10 ± 4	10 ± 4
Months since surgery	12 ± 4	12 ± 4
MDS UPDRS-III scores	34 ± 14	53 ± 16

Values are reported as mean ± standard deviation

DBS deep brain stimulation, *n* number of patients, MDS UPDRS-III Movement Disorder Society's Unified Parkinson's Disease Rating Scale-III

extracted from the Automated Anatomical Labeling atlas [24]) and were registered to each patient's 3D T1 MPRAGE images using the FMRIB Software Library (FSL, <https://fsl.fmrib.ox.ac.uk/fsl/fslwiki/>, version 5.0.11).

Tractography Reconstruction

Deterministic Tractography

Deterministic brute-force tractography was performed using Diffusion Toolkit (<http://trackvis.org>, version 0.6.4.1), a user-friendly cross-platform software, which allows interactive track data manipulation in real-time. Tracking was performed using a modified fiber assignment by continuous tracking (FACT) algorithm with a fractional anisotropy (FA) threshold of 0.2, angle threshold of 45°, orientation patch with *z* inverted and no swap, and default step length of 0.1 mm, which was found to produce the most anatomically accurate reconstruction [25]. Following the brute-force tract reconstruction, the TrackVis tract visualization program (<http://trackvis.org>, version 0.6.1) was automatically launched. The whole-brain tracks file and the ROIs were uploaded manually. The SN and STR were used as filters to partition the NSP. Similarly, those streamlines from the DN to the contralateral THA were retained as the estimates of the DRTT, and those

streamlines from the PG to the STN were retained as the estimates of the HDP. The tract counts shown in the Property-Track module were recorded.

Probabilistic Tracking

Probabilistic tractography of the NSP, DRTT, and HDP was performed using FSL's Protrackx 2.0. To resolve the issues of crossing fibers, a Markov chain Monte Carlo sample was built using BEDPOSTX (Bayesian Estimation of Diffusion Parameters Obtained using Sampling Techniques) implemented by FSL's Diffusion Toolbox in which the diffusion coefficient was modeled using a gamma distribution with a maximum of two fibers per voxel.

The default settings of Protrackx 2.0 were as follows: 5000 samples/voxel, step length = 0.5 mm, curvature threshold = 0.2, and "loopcheck" selected to ensure that no tracts were included that doubled back on themselves [26, 27]. The SN, DN, and PG cortical areas were set as the seed masks, and the STR, THA, and STN were set as termination targets, respectively. The number of streamlines propagating from the seeded regions to the targets was calculated for each voxel in this manner. As such, the resulting output map represented the robustness of the fiber tract, as described by the probability of its existence in a

particular voxel between the seed region and the termination target. The connection probability was defined as follows: mean number of streamlines per voxel sampled = sum of voxel values in the result map / number of voxels in the seed mask [27].

Clinical Outcome Measures

The Movement Disorder Society’s Unified Parkinson’s Disease Rating Scale-III (MDS UPDRS-III) was used for both preoperative motor symptom assessment (in the states of medication-on and medication-off) and postoperative assessment (in the states of medication-off/DBS-on and medication-off/DBS-off). The preoperative UPDRS-III scores were available for 28 patients. The postoperative UPDRS-III scores of the DBS-on state were available for all 31 patients. The postoperative UPDRS-III scores of the DBS-off state were available for 28 patients. The clinical efficacy was calculated using the following formula:

$$\text{Improvement} = \left(1 - \frac{\text{scores with DBS}_{\text{on}}}{\text{scores with DBS}_{\text{off}}} \right) \times 100\%.$$

The patients whose DBS-on state UPDRS-III scores decreased by at least 25% compared to those of the DBS-off state were defined as responders to DBS treatment, and the patients whose motor improvement was less than 25% were defined as nonresponders to DBS treatment.

VTA Estimation and Distance to Tracts

The location of DBS electrodes was reconstructed using the Lead-DBS toolbox (www.lead-dbs.org) by registration of the preoperative structural MR images and the postoperative CT scans. The stimulation parameters (i.e., the location of the active stimulation contacts and voltage amplitudes) were specified for each individual patient. The VTAs for each patient were then estimated using a finite element method (FEM) approach in Lead Group [8]. For further analysis, the center of gravity (COG) of

each white matter fiber track and the VTAs were calculated using the *regionprops3* function in MATLAB, defined as:

$$\begin{bmatrix} x_{\text{cog}} \\ y_{\text{cog}} \\ z_{\text{cog}} \end{bmatrix} = \frac{\sum_{i=1}^n m_i \times \begin{pmatrix} x_i \\ y_i \\ z_i \end{pmatrix}}{\sum_{i=1}^n m_i},$$

where $[x_{\text{cog}} y_{\text{cog}} z_{\text{cog}}]$ represents the coordinates of the COG, and m_i represents the value of each voxel i with its coordinates $[x_i y_i z_i]$ in the three-dimensional space. The resulting COG coordinates of the VTAs were transformed from the MNI space to the patients’ individual diffusion-weighted image using Advanced Normalization Tools (ANTs, <https://www.nitrc.org/projects/ants>, [28]). Subsequently, the Euclidean distances between the COGs of the right and left hemispheric STN VTAs and the COGs of the white matter fiber tracks (the resulting individual NSPs, DRTTs, and HDPs, in Sect. 2.5.2) were calculated.

Statistical Analysis

Statistical analyses were conducted using SPSS software (version 22.0, IBM Corp., Armonk, NY, USA). The differences in the volume and FA of the ROIs between the DBS-on and DBS-off states were compared using a paired t test. The differences in the numbers of tract count and the connection probability between the DBS-on and DBS-off states were compared using the Wilcoxon test. The differences in the numbers of tract count and the connection probabilities between the left and right sides were also compared using the Wilcoxon test. Pearson correlation analysis was performed to investigate the relationships between the baseline severity of the motor symptoms in the patients and the white matter tract connection probabilities. The distances from the VTAs to the tracts were compared between the responder group and non-responder group using the independent t test. Results with a p value < 0.05 were considered statistically significant.

RESULTS

Safety of DTI Scanning with Implanted DBS Device

The duration from the DBS implantation surgery to the post MRI session ranged from 4 to 102 months in the patients (Fig. S1). There were no adverse events related to the MRI. During the MR scanning in the DBS-on state, there was no disruption of the stimulation due to the DBS device being switched off unexpectedly.

Demonstration of DTI B_0 Images

The B_0 images of one representative patient in the DBS-on and DBS-off states, respectively, are shown in Fig. S2. The yellow arrows indicate artifacts generated by the extension cables which were placed on the skull, resulting in signal loss observed over the parietal and temporal regions of the left hemisphere. The red arrows indicate the artifacts generated by the DBS electrodes. The sequence with high bandwidth and short TE helped constrain the artifacts to the area near and around the metal materials.

Comparison of DTI Characteristics Between DBS-on and DBS-Off States

The segmentation outlines of the 12 ROIs in a representative patient are illustrated in Fig. S3. The mean values and standard deviations of the volume and the FA value of the ROIs are shown in Table S2. There was no significant difference in the volume or FA value of the defined seed and target ROIs between the DBS-on and the DBS-off states. The FA of the left SN was significantly lower than that of the right SN ($p < 0.05$ in both DBS-on and DBS-off states).

Tractography Delineation by Deterministic Tracking

Figure 2 shows the deterministic tracking result of one representative patient in two states: (a) DBS-on state and (b) DBS-off state. As seen in

the representative images, only a few tracts are identified by deterministic tracking.

For both the DBS-on and the DBS-off conditions of DTI, the NSP was successfully reconstructed in most of the patients (69.6–77.4%); the HDP was reconstructed in a small proportion of patients (4.3–12.9%), and the DRTT could not be reconstructed at all. The number and percentage of patients with successfully reconstructed tractography are shown in Table 2.

No significant differences were observed in the numbers of tract count of the right NSP versus that of the left NSP (DBS-on: $p = 0.183$; DBS-off: $p = 0.069$). The numbers of NSP tract count between the DBS-on and the DBS-off states show no statistical differences in either side (right side: $p = 0.476$; left side: $p = 0.563$) as shown in Table 3.

Tractography Delineation by Probabilistic Tracking

The probabilistic fiber tracking detected the NSP, DRTT, and HDP in all 62 hemispheres in the DBS-on state and in 46 hemispheres in the DBS-off state. Figure 3 shows the probabilistic tracking result of one representative patient in two states: (a) DBS-on state and (b) DBS-off state. Overall, the NSP is best reconstructed on the postoperative images, followed by the DRTT and the HDP, which is in concordance with the results by the DT method. It should be noted that the artifacts produced by DBS leads and electrode contacts in and around the STN to some extent lead to signal loss in DTI data, so the fibers between PG and STN cannot always be accurately reconstructed.

The connection probabilities of bilateral tracts in the DBS-on and DBS-off states are summarized in Table 4. There was no significant difference in the tracking results of the bilateral fiber bundles of NSP and DRTT between the DBS-on and the DBS-off conditions (right NSP: $p = 0.306$; left NSP: $p = 0.053$; right DRTT: $p = 0.503$; left DRTT: $p = 0.670$). The connection probabilities of the left NSP are significantly lower than those of the right side in both DBS-on and DBS-off states ($p < 0.05$ in both states).

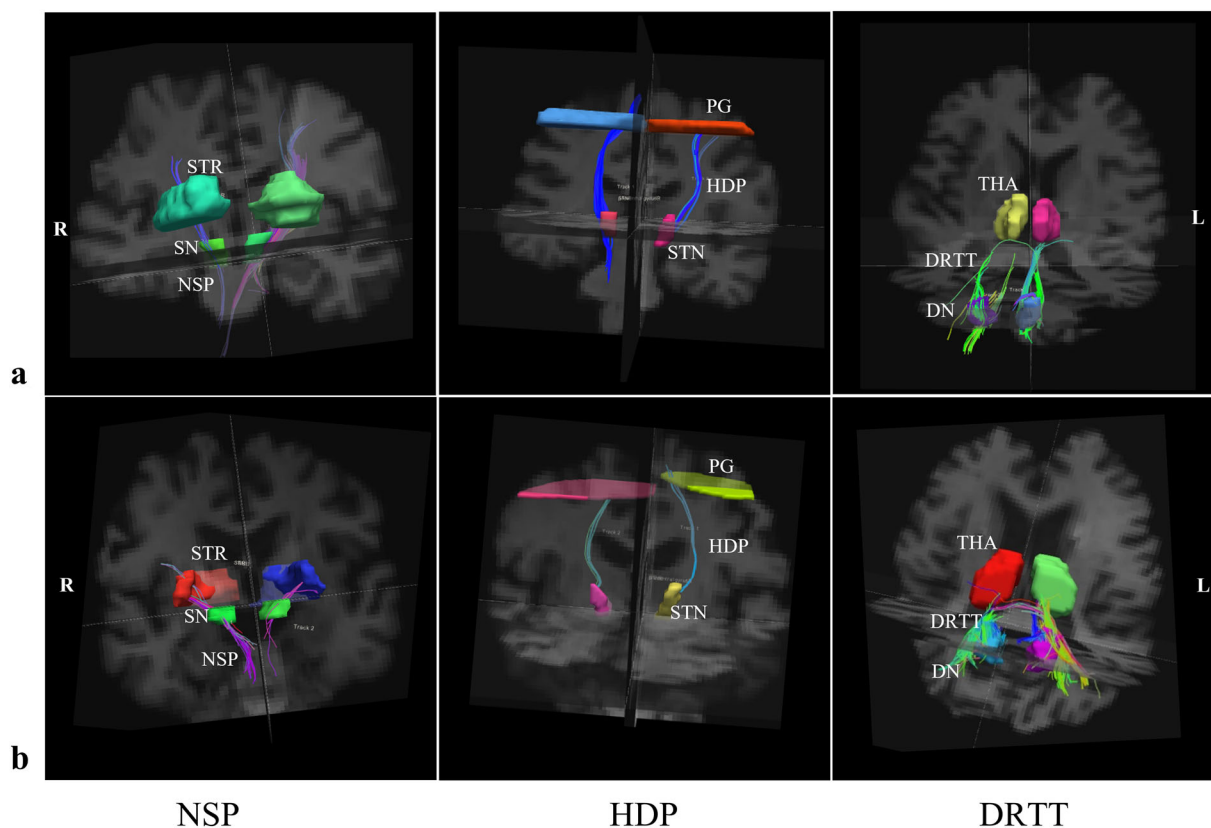


Fig. 2 Illustration of the NSP, HDP, and DRTT reconstructed by deterministic tracking method in one representative patient in two states. **a** DBS-on state; **b** DBS-off state. *STR* striatum, *THA* thalamus, *PG*

precentral gyrus, *SN* substantia nigra, *STN* subthalamic nucleus, *DN* dentate nucleus, *NSP* nigrostriatal pathway, *HDP* hyperdirect pathway, *DRTT* dentato-rubro-thalamic pathway

No significant differences were shown between the connection probabilities of bilateral DRTT (DBS-on: $p = 0.248$; DBS-off: $p = 0.879$).

In addition, a negative correlation was found between the preoperative UPDRS-III scores in the medication-on state and the connection probability of left NSP identified on the images in the DBS-on state ($r = -0.39$, $p = 0.042$, Fig. 4a). The correlation coefficient of the preoperative medication-on UPDRS-III scores against the connection probability of right NSP in the DBS-on state was not significant ($r = -0.25$, $p = 0.205$, Fig. 4b).

Relationship Between VTA–Bundles Distance and Clinical Improvement

As shown in Fig. 5a, the distance between the left VTA and the left NSP of responders was

significantly shorter compared to that of the non-responders (responder group: 4.2 ± 2.7 mm, non-responder group: 7.4 ± 5.2 mm, $p = 0.046$, equal variances assumed). The distance between the right VTA and the right NSP in the responsive group was not significantly different from that in the non-responsive group (responder group: 5.6 ± 3.0 mm, non-responder group: 6.3 ± 4.6 mm, $p = 0.672$, equal variances assumed, Fig. 5b).

DISCUSSION

Main Findings

The present work demonstrated, firstly, that a safe and feasible DTI sequence, which takes less

Table 2 The number (percentage) of patients whose white matter tracts were successfully reconstructed using deterministic tractography

Tracts	Side	DBS state	
		DBS-on (<i>n</i> = 31)	DBS-off (<i>n</i> = 23)
NSP	R	24 (77.4%)	16 (69.6%)
	L	23 (74.2%)	17 (73.9%)
HDP	R	4 (12.9%)	2 (8.7%)
	L	3 (9.7%)	1 (4.3%)
DRTT	R	0 (0%)	0 (0%)
	L	0 (0%)	0 (0%)

n number of patients, *R* right side, *L* left side, *NSP* nigrostriatal pathway, *HDP* hyperdirect pathway, *DRTT* dentato-rubro-thalamic pathway

than 10 min of scanning, can be performed in postoperative PD patients with on-state DBS in a 1.5-T scanner. The motor tracts near the STN, which are thought to be involved in the pathophysiology of PD, specifically the NSP, DRTT, and HDP, can be reconstructed using the DT or PT method. There was no significant difference in the fiber tracking results between the DBS-on and DBS-off DTI data. Secondly, the FA of the left SN and the connection probability of the left NSP were significantly lower than those of the right side, and the connection probability of the left NSP was negatively correlated with the preoperative UPDRS-III scores in the medication-on state, indicating the asymmetry of degeneration of the NSP in PD patients. Thirdly,

the distance between the left VTA and ipsilateral NSP was significantly shorter in the responders to DBS treatment than in the non-responders, indicating that clinically effective DBS electrodes are in close anatomical proximity to the NSP tracts.

Safety and Feasibility of the Postoperative DTI Approach

The treatment effect of DBS is associated with the electrical impact of DBS on the white matter tracts in the vicinity of the stimulation site [4, 5, 29, 30]. The DBS effect is altered years after implantation [13], which may result from the gradual degeneration of the white matter tracts. To understand the mechanisms, the safety and feasibility of the reconstruction of white matter tracts from the less common MRI sequence, namely DTI, need to be validated first. A recent study indicated that the white matter tracts can be successfully reconstructed from a 25-min DTI scan in the DBS-off state [15]. However, whether the white matter tracts can be successfully reconstructed from the DTI data acquired within a shorter amount of time in the DBS-on state remains unclear. A short acquisition time of postoperative imaging data and the scanning with DBS-on can significantly facilitate related research and clinical practice.

The DTI sequence adopted in this study proved to be safe and clinically feasible for two main reasons. First, the SAR value of the DTI sequence performed was only 0.34 ± 0.02 W/kg, which is lower than the recommended

Table 3 The tract numbers of the bilateral NSP in DBS-on and DBS-off states

Tracts	Side	DBS state		<i>p</i> value
		DBS-on (<i>n</i> = 31)	DBS-off (<i>n</i> = 23)	
NSP	R	13 (3, 79)	19 (8.5, 39)	0.476
	L	13 (1, 37)	9 (2.5, 35)	0.563
	<i>p</i> value	0.183	0.069	–

The tract count numbers are shown in the form of median (IQR1, IQR3)

n number of patients, *NSP* nigrostriatal pathway, *R* right side, *L* left side, *DBS* deep brain stimulation, *IQR* interquartile range

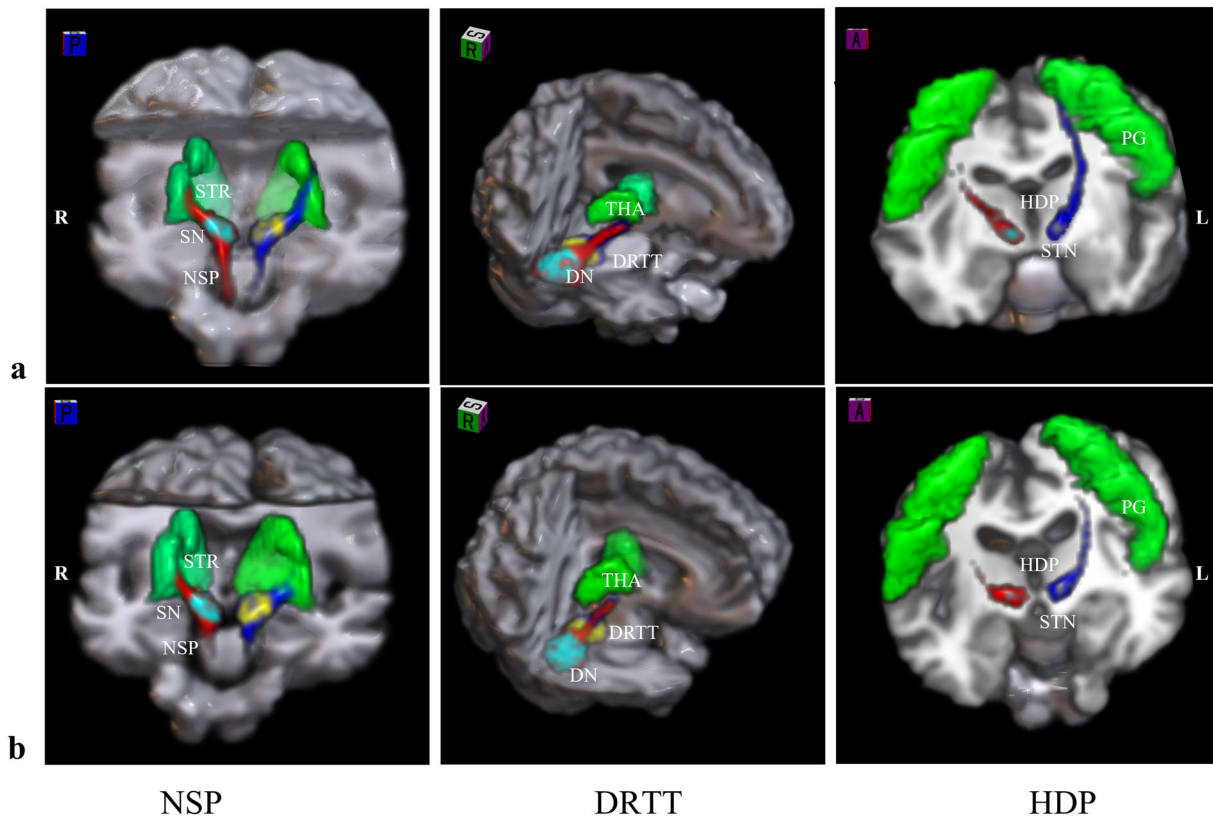


Fig. 3 Illustration of the NSP, DRTT, and HDP reconstructed by probabilistic tracking method in one representative patient in two states. **a** DBS-on state; **b** DBS-off state. *STR* striatum, *THA* thalamus, *PG* precentral gyrus, *SN* substantia nigra, *STN* subthalamic nucleus, *DN* dentate nucleus, *NSP* nigrostriatal pathway, *DRTT* dentato-rubro-thalamic pathway, *HDP* hyperdirect pathway

Table 4 The connection probabilities of the patients in DBS-on and DBS-off states

Tracts	Side	DBS state		<i>p</i> value
		DBS-on (<i>n</i> = 31)	DBS-off (<i>n</i> = 23)	
NSP	R	131 (115, 154)	125 (112, 156)	0.306
	L	118 (106, 133)	120 (110, 144)	0.053
	<i>p</i> value	< 0.001	0.001	–
DRTT	R	69 (59, 75)	68 (61, 75)	0.503
	L	71 (56, 77)	69 (62, 80)	0.670
	<i>p</i> value	0.248	0.879	–

Significant differences are in bold. The connection probabilities are shown in the form of median (IQR1, IQR3) *n* number of patients, *R* right side, *L* left side, *NSP* nigrostriatal pathway, *DRTT* dentato-rubro-thalamic pathway; IQR, interquartile range

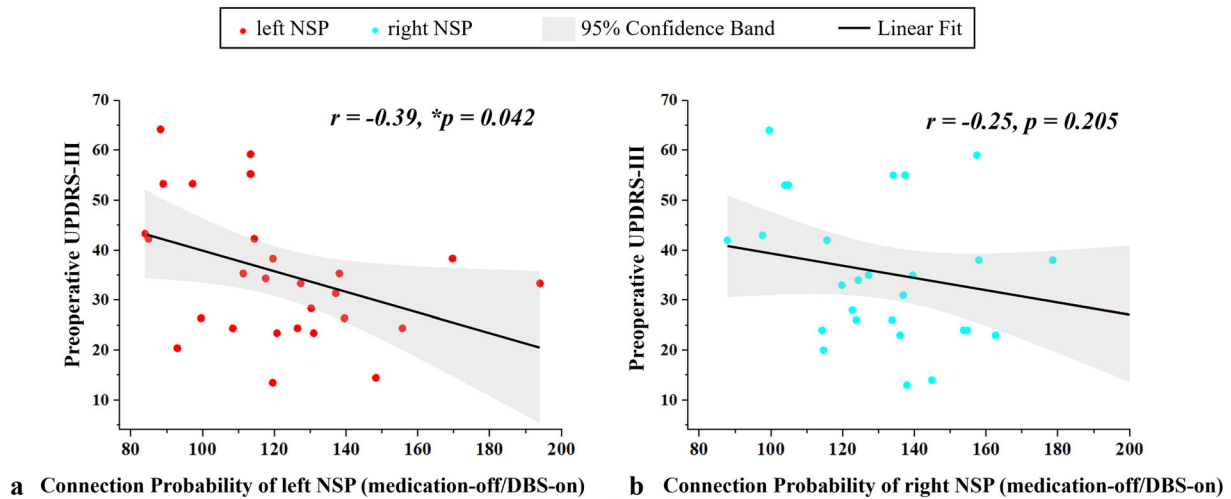


Fig. 4 Correlation between the preoperative UPDRS-III scores and the connection probability of NSP. **a** Correlation between UPDRS-III scores with the connection

probability of the left NSP; **b** correlation between UPDRS-III scores with the connection probability of the right NSP

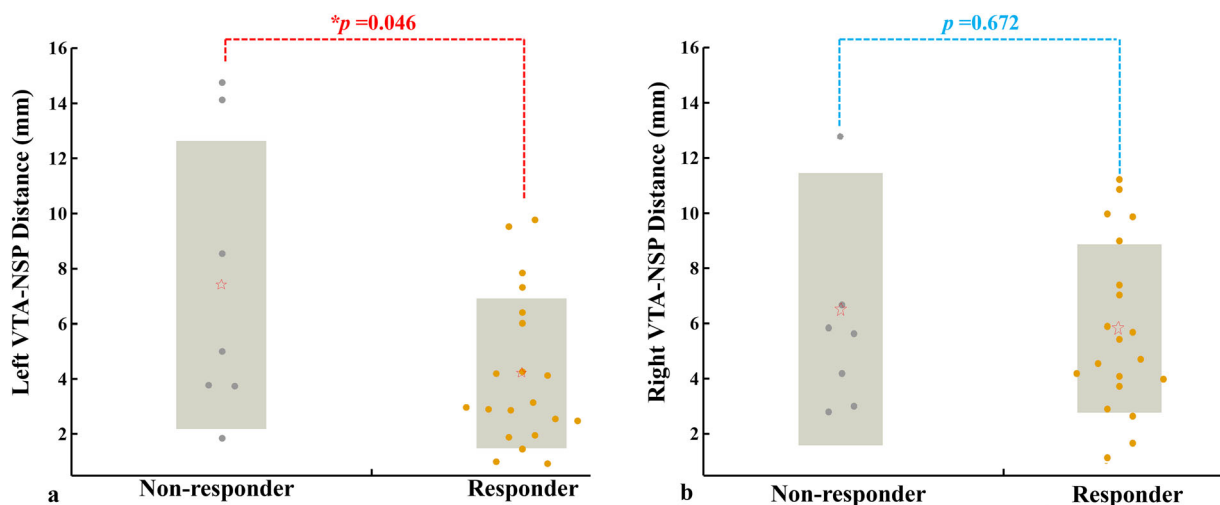


Fig. 5 Comparison of distances between VTA and NSP in responder and non-responder groups. **a** The left-side VTA–NSP distance of the responders is significantly shorter than that of the non-responders; **b** the right-side

VTA–NSP distance of the responders is not significantly different from that of the non-responders. *VTA* volumes of tissue activated, *NSP* nigrostriatal pathway

threshold level of 0.4 W/kg [19]. The SAR values of T1-weighted and T2-weighted sequences for the postoperative MR scanning have been proven safe in previous studies [31]. However, research on the safety of DTI sequences with DBS device implantation remains limited. Both our present study and a recent study [15]

suggest that scanning of DTI sequences with a DBS device is safe under a 1.5-T MR scanner.

As is known, the acquisition time of the DTI sequence is much longer than the clinically used T1WI and T2WI sequences [32]. The acquisition time of the DTI sequence in the present study was 9 min 13 s. We shortened the

total acquisition time by setting a relatively short repetition time (6500 ms) while keeping the SAR value under the recommended threshold level (0.4 W/kg) [19]. Compared with the recent study, in which it took about 25 min to acquire postoperative DTI images for tractography [15], our results show that clinically useful DTI images can be acquired within a relatively short amount of time. Given that the access to MR scanners in most centers is limited and that the long duration of scanning may make patients feel restless [33], the proposed 10-min scanning protocol in our study is more efficient and clinically practical than the 25-min protocol proposed in a previous study [15], which can facilitate the examination of the white matter tracts around the stimulation contacts in future research.

Artifacts in the DTI Image with a DBS Device

There have been concerns regarding the effect of MRI on surgically implanted metal electrodes due to possible heating and displacement of the metal components by the magnet [31, 34–36]. Nevertheless, postoperative DTI is a useful imaging modality for patients with PD or other movement disorders, since it has the capability to show both the electrode position and the white matter tracts on the same image. A safe DTI approach in both DBS-on and DBS-off states would make it possible to carry out longitudinal studies exploring the relationship between DBS location and the surrounding white matter bundles in a variety of diseases.

As indicated by a recent study, the delineation of tracts in postoperative imaging decreases compared with that in preoperative imaging due to susceptibility artifacts [15]. In our study, susceptibility artifacts and the quality of the DTI images were assessed visually. The susceptibility artifacts were generated by the fixing caps, connector wires, extension cables, and the DBS electrodes, resulting in signal loss over the parietal and temporal lobes on the right hemisphere. The precise characteristics of the artifact induced by the DBS electrodes have been fully described by Li and colleagues [18].

In this study, a spin-echo sequence was applied to help constrain the artifacts to the area near and around the metal materials. The results showing that the white matter tracts could be successfully delineated in most patients suggest that the metal artifacts are not so significant to have a vital influence on the tractography reconstruction.

Influence of Electrical Pulses on Postoperative Tractography Construction

Both the DT method and the PT method have been extensively applied in clinical neuroscience studies to explore the nervous system architecture of PD patients [37], but few papers have reported the postoperative tractography comparison between the DBS-on and DBS-off states. Notably, Muller and colleagues only tested the feasibility of the reconstruction of the white matter bundles in the DBS-off state [15]. We additionally tested the reconstruction in the DBS-on state. Our results show no difference in the volume or FA of the predefined seeds and target ROIs between the DBS-on and DBS-off conditions. Moreover, the numbers of white matter tracts and the connection probabilities show no statistical differences on either side between the DBS-on and the DBS-off states. Our results suggest that tractography based on DTI is not affected by the high-frequency electrical pulses sent to the deep brain nuclei through the implanted electrodes. MR scanning in the DBS-on state can benefit those postoperative patients who cannot control their disease symptoms without stimulation.

Asymmetry of the SN and NSP

As shown in Sects. 3.3 and 3.5, the FA of the left SN and the connection probabilities of the left NSP were significantly lower than those on the right side. Asymmetry in FA of the SN in PD patients has also been reported in other studies, which is implicated in an asymmetrical degeneration of dopaminergic nigral neurons. While some studies indicate that the asymmetry of FA of the SN correlates with the clinical asymmetry

in PD patients [38], others report no such association [39, 40]. For instance, Prakash and colleagues [39] found that the FA was lower at the left rostral SN compared to the right SN, regardless of the motor asymmetry. Safai and colleagues also reported that the FA in the left SN was significantly lower than that in the right SN, with no details pertaining to clinical laterality [40]. In our study, the FA of the left SN and the connection probability of the left NSP were significantly lower than those of the right side, which is consistent with the hypotheses of inherently lower dopamine levels in the left than the right NSP and/or the higher vulnerability of the left NSP to pathogenetic mechanisms underlying PD [41], although further studies are needed to better understand the mechanisms underlying asymmetric nigrostriatal features in PD.

Our results highlight the asymmetry in FA and connection probabilities that can be revealed in PD patients implanted with a DBS device. Notably, the result of asymmetry was only revealed by the PT method and not the DT method, probably because PT is more sensitive in detecting complex crossing fibers than DT [42]. Moreover, the connection probability of left NSP showed a significant negative correlation with the preoperative UPDRS-III motor scores. Such results are consistent with the observations from a previous study by Andica and colleagues [43], suggesting that impaired motor function is related to axonal degeneration in PD patients.

Positional Relationship Between the Clinically Effective DBS Electrodes and the NSP Tracts

Another clinical finding in our study is that the distance from the left VTA to the left NSP was significantly shorter in the DBS-responder group compared to the DBS-non-responder group. The efferent from the STR to the SN, known as the nigrostriatal pathway, seems to play a critical role in movement disorders, as it is severely affected by neurodegeneration in PD patients [44]. A close association between the distance of white matter tracts from the

stimulation site and the DBS effect has been observed in patients with essential tremor [30] and dystonia [29], and our findings suggest such an implication in the treatment of STN-DBS for Parkinson's disease as well. The degeneration of the nigrostriatal system is the neural basis for PD [44]. A recent animal study indicated that STN-DBS induced sustained neurorestorative effects in the nigrostriatal system [45], suggesting that the nigrostriatal system is involved in the therapeutic mechanisms of DBS in PD. Our findings indicate that the impact of DBS on the nigrostriatal system, namely NSP, is strongly associated with the treatment effect of motor symptoms in PD, which may help to optimize electrode placement and postoperative electrode contact selection. A symptom-specific and connectivity-based approach for target planning and postoperative parameter setting for DBS may improve the treatment outcomes and reduce adverse effects [46], and imaging of the structural connectivity in postoperative patients would facilitate longitude studies on the relationships among the DBS location, white matter profile, and clinical effect.

It is important to assess the possible clinical outcome of DBS before implantation, and thus DTI before the operation is strongly recommended. Nevertheless, PD is a progressive disease, and the structural connections may be gradually altered months or years after DBS implantation, which might be associated with a decline in the DBS effect years later [13]. DTI after the operation can provide information that may elucidate the related mechanisms. In this study, our primary focus was to map the motor pathways near the STN in PD patients with implanted DBS devices and examine the relationship between the characteristics of the reconstructed white matter tracts and motor symptoms. We have confirmed that the postoperative effect of DBS is related to the distance from the left VTAs by STN-DBS to the ipsilateral NSP. Postoperative DTI may help elucidate the mechanisms related to alterations of the DBS effect after implantation.

Limitations and Future Directions

This study has several limitations. First, the reconstruction of white matter tractography is time-consuming and requires specialized analysis and skills that may limit its clinical application. A more efficient and user-friendly data processing pipeline is needed for clinicians to evaluate the pathways influenced by DBS. Second, high-field MRI at 3.0-T is superior for optimal diffusion tensor imaging and white matter fiber tractography due to its superior signal-to-noise ratio. However, current manufacturer guidelines restrict scanning of patients with implanted DBS to field strengths no greater than 1.5-T. The potential risk of heating at the implanted electrodes due to induced voltage in the DBS device from the interactions with the applied radiofrequency (RF) field could theoretically result in thermal lesions in the tissue adjacent to the electrodes and cause serious physical harm to the patients [47]. Thus, efforts should be made towards SAR reduction in clinical practice for safe imaging with 3.0-T MR scanners in patients implanted with DBS. Third, the small sample size, especially the small number of non-responsive patients, undermines the statistical power of the present study, and thus the related clinical findings need to be replicated in a larger patient group in the future.

PD has been associated with progressive neuronal degeneration in the SN as well as the related white matter tracts. Our findings may provide a technical reference for the longitudinal postoperative tracking of patients with DBS to elucidate the relationship between alterations in white matter pathways and the long-term effects of DBS. Although our primary focus of this study was to map the motor pathways near the STN in PD patients with an implanted DBS device and to examine the relationship between the characteristics of the reconstructed white matter tracts and motor symptoms, tractography based on DTI in postoperative patients may also facilitate the study of the neural mechanism for the non-motor aspects of PD. Since non-motor symptoms such as affective disorders and cognition decline are common in advanced PD patients [48], and because STN-DBS may influence the affective and cognitive

processes through the structural connections with a variety of related cortical and subcortical areas [5, 49, 50], future studies are recommended to explore the relationship between non-motor symptoms and tractography in the patients with a DBS device based on DTI.

CONCLUSION

The safety of postoperative DTI with DBS-on state and the feasibility of reconstruction of the white matter tracts in the vicinity of the stimulation site of STN-DBS are validated in the present study. The asymmetry of the axonal system in PD patients, namely the asymmetry of the FA in SN and the connection probabilities of NSP, is confirmed based on the postoperative DTI images. Our findings also highlight the association between the impact of DBS-on NSP and the treatment effect of motor symptoms in PD. White matter fiber tractography based on DTI provides a promising tool to strengthen our understanding of the pathophysiology of Parkinson's disease and the therapeutic mechanisms underlying DBS treatment. Tractography imaging after DBS implantation may also help guide individualized DBS parameter programming postoperatively, and may facilitate the study of non-motor symptoms in PD patients with DBS.

ACKNOWLEDGEMENTS

We would like to thank all the participants of the study, and we are grateful to all the research assistants who offered their help in this study.

Funding. This study was supported and funded by the National Natural Science Foundation of China (81971576 and 81801652) and the Innovative Research Team of High-level Local Universities in Shanghai, which directly support our study on Parkinson's disease. The National Natural Science Foundation of China (81971576) provided funding for the journal's Rapid Service Fee.

Authorship. All named authors meet the International Committee of Medical Journal Editors (ICMJE) criteria for authorship for this article, take responsibility for the integrity of the work as a whole, and have given their approval for this version to be published.

Author Contributions. Yan Li: conceptualization, methodology, formal analysis, investigation, data curation, and writing-original draft. Naying He: investigation, validation, funding acquisition, and writing-review and editing. Chencheng Zhang: conceptualization, validation, and writing-review and editing. Yu Liu: data curation and investigation. Jun Li: writing-review and editing. Bomin Sun: resources and investigation. Yijie Lai: data curation and investigation. Hongyang Li: data curation and investigation. Chengyan Wang: validation and writing-review and editing. Ewart Mark Haacke: conceptualization, supervision, and writing-review and editing. Fuhua Yan: resources, supervision, project administration, and funding acquisition. Dianyou Li: resources, conceptualization, supervision, and writing-review and editing.

Disclosures. Yan Li, Naying He, Chencheng Zhang, Yu Liu, Jun Li, Bomin Sun, Yijie Lai, Hongyang Li, Chengyan Wang, Ewart Mark Haacke, Fuhua Yan and Dianyou Li declare that they have no known competing financial interests or personal relationships that could have appeared to influence the work reported in this paper.

Compliance with Ethics Guidelines. This study was approved by the Ruijin Hospital Institutional Review Board (Approval Number: 2018017). All procedures in the present study were in accordance with the Declaration of Helsinki. Each patient was informed of the procedures of the study and signed a consent form. The data collected in this study were de-identified. No identifiable protected health information was extracted or accessed during the study, which is compliant with the Health Insurance Portability and Accountability Act (HIPAA).

Data Availability. The datasets generated during and/or analyzed during the current study are available from the corresponding author on reasonable request.

Open Access. This article is licensed under a Creative Commons Attribution-NonCommercial 4.0 International License, which permits any non-commercial use, sharing, adaptation, distribution and reproduction in any medium or format, as long as you give appropriate credit to the original author(s) and the source, provide a link to the Creative Commons licence, and indicate if changes were made. The images or other third party material in this article are included in the article's Creative Commons licence, unless indicated otherwise in a credit line to the material. If material is not included in the article's Creative Commons licence and your intended use is not permitted by statutory regulation or exceeds the permitted use, you will need to obtain permission directly from the copyright holder. To view a copy of this licence, visit <http://creativecommons.org/licenses/by-nc/4.0/>.

REFERENCES

1. Shahidi GA, Rohani M, Parvareh M, Haghi-Ash-tiani B, Saeedi M, Rashedi R, et al. Outcome of subthalamic nucleus deep brain stimulation on long-term motor function of patients with advanced Parkinson disease. *Iran J Neurol*. 2017;16:107–11.
2. Tsai ST, Hung HY, Hsieh TC, Lin SH, Lin SZ, Chen SY. Long-term outcome of young onset Parkinson's disease after subthalamic stimulation—a cross-sectional study. *Clin Neurol Neurosurg*. 2013;115:2082–7. <https://doi.org/10.1016/j.clineuro.2013.07.014>.
3. Zibetti M, Merola A, Rizzi L, Ricchi V, Angrisano S, Azzaro C, et al. Beyond nine years of continuous subthalamic nucleus deep brain stimulation in Parkinson's disease. *Mov Disord*. 2011;26:2327–34. <https://doi.org/10.1002/mds.23903>.
4. Vassal F, Dilly D, Boutet C, Bertholon F, Charier D, Pommier B. White matter tracts involved by deep brain stimulation of the subthalamic nucleus in Parkinson's disease: a connectivity study based on preoperative diffusion tensor imaging tractography.

- Br J Neurosurg. 2020;34:187–95. <https://doi.org/10.1080/02688697.2019.1701630>.
5. Vanegas-Arroyave N, Lauro PM, Huang L, Hallett M, Horovitz SG, Zaghoul KA, et al. Tractography patterns of subthalamic nucleus deep brain stimulation. *Brain*. 2016;139:1200–10. <https://doi.org/10.1093/brain/aww020>.
 6. Coenen VA, Allert N, Paus S, Kronenbürger M, Urbach H, Mädler B. Modulation of the cerebello-thalamo-cortical network in thalamic deep brain stimulation for tremor: a diffusion tensor imaging study. *Neurosurgery*. 2014;75:657–69. <https://doi.org/10.1227/NEU.0000000000000540>.
 7. Antal M, Beneduce BM, Regehr WG. The substantia nigra conveys target-dependent excitatory and inhibitory outputs from the basal ganglia to the thalamus. *J Neurosci*. 2014;34:8032–42. <https://doi.org/10.1523/JNEUROSCI.0236-14.2014>.
 8. Akram H, Surg FN, Sotiropoulos SN, Jbabdi S. Subthalamic deep brain stimulation sweet spots and hyperdirect cortical connectivity in Parkinson's disease. *Neuroimage*. 2017;44:332–45. <https://doi.org/10.1016/j.neuroimage.2017.07.012>.
 9. Iarkov A, Barreto GE, Grizzell JA, Echeverria V. Strategies for the treatment of Parkinson's disease: beyond dopamine. *Front Aging Neurosci*. 2020;12:1–20. <https://doi.org/10.3389/fnagi.2020.00004>.
 10. Hamani C, Florence G, Heinsen H, Plantinga BR, Temel Y, Uludag K, et al. Subthalamic nucleus deep brain stimulation: Basic concepts and novel perspectives. *ENeuro*. 2017. <https://doi.org/10.1523/ENEURO.0140-17.2017>.
 11. Horn A, Reich M, Vorwerk J, Li N, Wenzel G, Fang Q. Connectivity predicts deep brain stimulation outcome in Parkinson disease contributed to the acquisition and analysis of data. *Ann Neurol*. 2017;82:67–78. <https://doi.org/10.1002/ana.24974>. [Connectivity](https://doi.org/10.1002/ana.24974).
 12. Wang Q, Akram H, Muthuraman M, Gonzalez-Escamilla G, Sheth SA, Oxenford S, et al. Normative vs. patient-specific brain connectivity in deep brain stimulation. *Neuroimage*. 2021;224:117307. <https://doi.org/10.1016/j.neuroimage.2020.117307>.
 13. Aviles-Olmos I, Kefalopoulou Z, Tripoliti E, Candelario J, Akram H, Martinez-Torres I, et al. Long-term outcome of subthalamic nucleus deep brain stimulation for Parkinson's disease using an MRI-guided and MRI-verified approach. *J Neurol Neurosurg Psychiatry*. 2014;85:1419–25. <https://doi.org/10.1136/jnnp-2013-306907>.
 14. Rodrigues NB, Mithani K, Meng Y, Lipsman N, Hamani C. The emerging role of tractography in deep brain stimulation: basic principles and current applications. *Brain Sci*. 2018. <https://doi.org/10.3390/brainsci8020023>.
 15. Muller J, Alizadeh M, Li L, Thalheimer S, Matias C, Tantawi M, et al. Feasibility of diffusion and probabilistic white matter analysis in patients implanted with a deep brain stimulator. *NeuroImage Clin*. 2020. <https://doi.org/10.1016/j.nicl.2019.102135>.
 16. See AAQ, King NKK. Improving surgical outcome using diffusion tensor imaging techniques in deep brain stimulation. *Front Surg*. 2017;4:1–11. <https://doi.org/10.3389/fsurg.2017.00054>.
 17. Saleh C, Doooms G, Berthold C, Hertel F. Post-operative imaging in deep brain stimulation: a controversial issue. *Neuroradiol J*. 2016;29:244–9. <https://doi.org/10.1177/1971400916639960>.
 18. Li Y, Buch S, He N, Zhang C, Zhang Y, Wang T, et al. Imaging patients pre and post deep brain stimulation: localization of the electrodes and their targets. *Magn Reson Imaging*. 2021;75:34–44. <https://doi.org/10.1016/j.mri.2020.09.016>.
 19. Larson PS, Richardson RM, Starr PA, Martin AJ. Magnetic resonance imaging of implanted deep brain stimulators: experience in a large series. *Stereotact Funct Neurosurg*. 2008;86:92–100. <https://doi.org/10.1159/000112430>.
 20. Horn A, Li N, Dembek TA, Kappel A, Boulay C, Ewert S, et al. Lead-DBS v2: towards a comprehensive pipeline for deep brain stimulation imaging. *Neuroimage*. 2019;184:293–316. <https://doi.org/10.1016/j.neuroimage.2018.08.068>.
 21. Roalf DR, Quarmley M, Elliott MA, Satterthwaite TD, Vandekar SN, Ruparel K, et al. The impact of quality assurance assessment on diffusion tensor imaging outcomes in a large-scale population-based cohort. *Neuroimage*. 2016;125:903–19. <https://doi.org/10.1016/j.neuroimage.2015.10.068>.
 22. Keuken MC, Backhouse PLBK, Himmer SBL. Effects of aging on T₁, T₂, and QSM MRI values in the subcortex. *Brain Struct Funct*. 2017;222:2487–505. <https://doi.org/10.1007/s00429-016-1352-4>.
 23. He N, Langley J, Huddleston DE, Ling H, Xu H, Liu C, et al. Improved neuroimaging atlas of the dentate nucleus. *Cerebellum*. 2017;16:951–6. <https://doi.org/10.1007/s12311-017-0872-7>.
 24. Rolls ET, Huang CC, Lin CP, Feng J, Joliot M. Automated anatomical labelling atlas 3. *Neuroimage*. 2020;206:116189. <https://doi.org/10.1016/j.neuroimage.2019.116189>.

25. Cui Z, Zhong S, Xu P, He Y, Gong G. PANDA: a pipeline toolbox for analyzing brain diffusion images. *Front Hum Neurosci.* 2013;7:42. <https://doi.org/10.3389/fnhum.2013.00042>.
26. Vaillancourt DE, Prodoehl J, Abraham I, Corcos DM, Zhou XJ, Cornelia CL, et al. High-resolution diffusion tensor imaging in the substantia nigra of de novo Parkinson disease. *Neurology.* 2009;72:1378–84. <https://doi.org/10.1212/01.wnl.0000340982.01727.6e>.
27. Theisen F, Leda R, Pozorski V, Oh JM, Adluru N, Wong R, et al. Evaluation of striatonigral connectivity using probabilistic tractography in Parkinson's disease. *NeuroImage Clin.* 2017;16:557–63. <https://doi.org/10.1016/j.nicl.2017.09.009>.
28. Avants BB, Epstein CL, Grossman M, Gee JC. Symmetric diffeomorphic image registration with cross-correlation: evaluating automated labeling of elderly and neurodegenerative brain. *Med Image Anal.* 2008;12:26–41. <https://doi.org/10.1016/j.media.2007.06.004>.
29. Rozanski VE, da Silva NM, Ahmadi SA, Mehrkens J, da Silva CJ, Houde JC, et al. The role of the pallidothalamic fibre tracts in deep brain stimulation for dystonia: a diffusion MRI tractography study. *Hum Brain Mapp.* 2017;38:1224–32. <https://doi.org/10.1002/hbm.23450>.
30. Anderson JS, Dhatt HS, Ferguson MA, Lopez-Larson M, Schrock LE, House PA, Deborah Y-T. Functional connectivity targeting for deep brain stimulation in essential tremor. *Am J Neuroradiol.* 2011;32:1963–8. <https://doi.org/10.3174/ajnr.A2638>.
31. Boutet A, Chow CT, Narang K, Elias GJB, Neudorfer C, Germann J, et al. Improving safety of MRI in patients with deep brain stimulation devices. *Radiology.* 2020;296:250–62. <https://doi.org/10.1148/radiol.2020192291>.
32. Soares JM, Marques P, Alves V, Sousa N. A hitchhiker's guide to diffusion tensor imaging. *Front Neurosci.* 2013;7:1–14. <https://doi.org/10.3389/fnins.2013.00031>.
33. Yamada K, Sakai K, Akazawa K, Yuen S, Nishimura T. MR tractography: a review of its clinical applications. *Magn Reson Med Sci.* 2009;8:165–74. <https://doi.org/10.2463/mrms.8.165>.
34. Rezaei AR, Baker KB, Tkach JA, Phillips M, Hrdlicka G, Sharan AD, et al. Is magnetic resonance imaging safe for patients with neurostimulation systems used for deep brain stimulation? *Neurosurgery.* 2005;57:1056–60. <https://doi.org/10.1227/01.NEU.0000186935.87971.2a>.
35. Chhabra V, Sung E, Mewes K, Bakay RAE, Abosch A, Gross RE. Safety of magnetic resonance imaging of deep brain stimulator systems: a serial imaging and clinical retrospective study: clinical article. *J Neurosurg.* 2010;112:497–502. <https://doi.org/10.3171/2009.7.JNS09572>.
36. Zrinzo L, Yoshida F, Hariz MI, Thornton J, Foltynie T, Yousry TA, et al. Clinical safety of brain magnetic resonance imaging with implanted deep brain stimulation hardware: large case series and review of the literature. *World Neurosurg.* 2011;76:164–72. <https://doi.org/10.1016/j.wneu.2011.02.029>.
37. Zhang Y, Burock MA. Diffusion tensor imaging in Parkinson's disease and Parkinsonian syndrome: a systematic review. *Front Neurol.* 2020;11:1–25. <https://doi.org/10.3389/fneur.2020.531993>.
38. Wang J, Yang QX, Sun X, Vesek J, Mosher Z, Vasavada M, et al. MRI evaluation of asymmetry of nigrostriatal damage in the early stage of early-onset Parkinson's disease. *Park Relat Disord.* 2015;21:590–6. <https://doi.org/10.1016/j.parkreldis.2015.03.012>.
39. Prakash BD, Sitoh YY, Tan LCS, Au WL. Asymmetrical diffusion tensor imaging indices of the rostral substantia nigra in Parkinson's disease. *Park Relat Disord.* 2012;18:1029–33. <https://doi.org/10.1016/j.parkreldis.2012.05.021>.
40. Safai A, Prasad S, Chougule T, Saini J, Pal PK, Ingahalikar M. Microstructural abnormalities of substantia nigra in Parkinson's disease: a neuromelanin sensitive MRI atlas based study. *Hum Brain Mapp.* 2020;41:1323–33. <https://doi.org/10.1002/hbm.24878>.
41. Scherfler C, Seppi K, Mair KJ, Donnemiller E, Virgolini I, Wenning GK, et al. Left hemispheric predominance of nigrostriatal dysfunction in Parkinson's disease. *Brain.* 2012;135:3348–54. <https://doi.org/10.1093/brain/aws253>.
42. Lim JC, Phal PM, Desmond PM, Nichols AD, Kokkinos C, Danesh-Meyer HV, et al. Probabilistic MRI tractography of the optic radiation using constrained spherical deconvolution: a feasibility study. *PLoS ONE.* 2015;10: e0118948. <https://doi.org/10.1371/journal.pone.0118948>.
43. Andica C, Kamagata K, Hatano T, Saito Y, Uchida W, Ogawa T, et al. Neurocognitive and psychiatric disorders-related axonal degeneration in Parkinson's disease. *J Neurosci Res.* 2020;98:936–49. <https://doi.org/10.1002/jnr.24584>.
44. Kordower JH, Olanow CW, Dodiya HB, Chu Y, Beach TG, Adler CH, et al. Disease duration and the integrity of the nigrostriatal system in Parkinson's

- disease. *Brain*. 2013;136:2419–31. <https://doi.org/10.1093/brain/awt192>.
45. Fauser M, Ricken M, Markert F, Weis N, Schmitt O, Gimsa J, et al. Subthalamic nucleus deep brain stimulation induces sustained neurorestoration in the mesolimbic dopaminergic system in a Parkinson's disease model. *Neurobiol Dis*. 2021;156:105404. <https://doi.org/10.1016/j.nbd.2021.105404>.
46. Strotzer QD, Kohl Z, Anthofer JM, Faltermeier R, Schmidt NO, Torka E, Greenlee MW, Fellner C, Schlaier JRBA. Structural connectivity patterns of side effects induced by subthalamic deep brain stimulation for Parkinson's disease. *Brain Connect*. 2021. <https://doi.org/10.1089/brain.2021.0051>.
47. Sammartino F, Krishna V, Sankar T, Fisico J, Kalia SK, Hodaie M, et al. 3-Tesla MRI in patients with fully implanted deep brain stimulation devices: a preliminary study in 10 patients. *J Neurosurg*. 2017;127:892–8. <https://doi.org/10.3171/2016.9.JNS16908>.
48. Poewe W. Non-motor symptoms in Parkinson's disease. *Eur J Neurol*. 2008;15:14–20. <https://doi.org/10.1111/j.1468-1331.2008.02056.x>.
49. Mosley PE, Robinson K, Coyne T, Silburn P, Barker MS, Breakspear M, et al. Subthalamic deep brain stimulation identifies frontal networks supporting initiation, inhibition and strategy use in Parkinson's disease. *Neuroimage*. 2020;223:117352. <https://doi.org/10.1016/j.neuroimage.2020.117352>.
50. Min HK, Hwang SC, Marsh MP, Kim I, Knight E, Strierner B, et al. Deep brain stimulation induces BOLD activation in motor and non-motor networks: an fMRI comparison study of STN and EN/GPi DBS in large animals. *Neuroimage*. 2012;63:1408–20. <https://doi.org/10.1016/j.neuroimage.2012.08.006>.